IEICE TRANSACTIONS

on Communications

VOL. E102-B NO. 6
JUNE 2019

A PUBLICATION OF THE COMMUNICATIONS SOCIETY

The Institute of Electronics, Information and Communication Engineers
Kikai-Shinko-Kaikan Bldg., 5-8, Shibakoen 3chome, Minato-ku, TOKYO, 105-0011 JAPAN

IEICE TRANS. COMMUN., VOL.E102–B, NO.6 JUNE 2019

PAPER *Special Section on Healthcare, Medical Information and Communication Technology for Safe and Secure Society*

Non-Contact Instantaneous Heart Rate Extraction System Using 24-GHz Microwave Doppler Sensor

Shintaro IZUMI[†a)], ***Member***, **Takaaki OKANO**[††], **Daichi MATSUNAGA**[††], ***Nonmembers***, **Hiroshi KAWAGUCHI**[††], ***Member***, ***and*** **Masahiko YOSHIMOTO**[††], ***Fellow***

SUMMARY This paper describes a non-contact and noise-tolerant heart rate monitoring system using a 24-GHz microwave Doppler sensor. The microwave Doppler sensor placed at some distance from the user's chest detects the small vibrations of the body surface due to the heartbeats. The objective of this work is to detect the instantaneous heart rate (IHR) using this non-contact system in a car, because the possible application of the proposed system is a driver health monitoring based on heart rate variability analysis. IHR can contribute to preventing heart-triggered disasters and to detect mental stress state. However, the Doppler sensor system is very sensitive and it can be easily contaminated by motion artifacts and road noise especially while driving. To address this problem, time-frequency analysis using the parametric method and template matching method are employed. Measurement results show that the Doppler sensor, which is pasted on the clothing surface, can successfully extract the heart rate through clothes. The proposed method achieves 13.1-ms RMS error in IHR measurements conducted on 11 subjects in a car on an ordinary road.

key words: *Burg's method, heart rate variability, instantaneous heart rate (IHR), microwave Doppler sensor, non-contact*

1. Introduction

The aging population in developed countries in recent years demands urgency of efforts to reduce health care costs. Prevention of lifestyle-related diseases including heart diseases such as myocardial infarction can be achieved through early detection and proper treatment. Preventing lifestyle-related diseases can be done by constantly monitoring physiological information. We specifically examined instantaneous heart rate (IHR) information, which is particularly important for human beings. The IHR and heart rate variability are useful indices for cardiac disease detection, stress monitoring, active mass monitoring, and so on.

Heart attack during driving has been a social problem because it causes serious accident. The number of patients with cardiovascular disease increases with progress of an aging society. Therefore, this paper focuses on the IHR monitoring in a car using a wearable sensor.

Electrocardiography (ECG), the standard method of heart rate measurement, can be done even in daily life using a traditional Holter monitor or a wearable ECG sensor [1]–[3]. Photoplethysmogram (PPG) sensor is also used for monitoring in daily life [4], [5]. As shown in Fig. 1, the IHR is obtained from the peak interval of heartbeat contained in ECG or PPG.

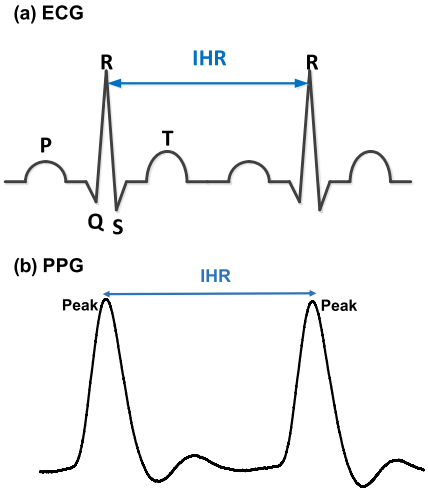

Fig. 1 IHR example in (a) ECG and (b) PPG waveforms.

However, because all entail physical burdens, they present the problem that they are unsuitable for constant monitoring of physiological information. Although, a lot of wearable sensor devices have been developed for ECG and heart rate measurement, these systems require pasting of wet electrodes directly onto the skin and thus poor usability. Therefore, the motivation of this work is non-contact IHR monitoring.

To realize remote heart rate monitoring, microwave Doppler sensors [6]–[12] were proposed to detect the heart velocity. Imaging-based methods using the color change of the face, which indicates the pulse beat, have also been proposed [13]. Although these methods present severe noise contamination problems, the heart rate can be detected without direct skin contact. For this work, we chose a 24-GHz microwave Doppler sensor as the remote heart rate monitor, because it has enough time resolution to detect IHR.

The microwave Doppler sensor can detect heartbeats from the imperceptible vibration of the human body surface caused by cardiac vibration. Unfortunately, the microwave Doppler sensor is very sensitive and it can be easily contaminated by body motion artifacts. A road noise also becomes a serious problem while driving. To prevent these

Manuscript received July 2, 2018.
Manuscript revised October 22, 2018.
Manuscript publicized December 19, 2018.
[†]The author is with Institute of Scientific and Industrial Research, Osaka University, Ibaraki-shi, 567-0047 Japan.
[††]The authors are with the Graduate School of System Informatics, Kobe University, Kobe-shi, 657-8501 Japan.
a) E-mail: shin@sanken.osaka-u.ac.jp
DOI: 10.1587/transcom.2018HMP0007

problems, time-frequency domain analysis using AR model based method and template matching method are introduced in this work. In a preliminary work [14], we reported that time frequency analysis is effective against noise contamination. This paper presents additional details of implementation and performance evaluation results. The proposed system is evaluated in a car while driving on an ordinary road, whereas the preliminary work described on a basic evaluation in the laboratory.

This paper is structured as follows. Section 2 of this report explains that how the microwave Doppler sensor detect the heartbeat, and the influence of the noise contamination. The time-frequency analysis method and detailed analysis of heart rate components with microwave Doppler sensor are described in Sect. 3. The influence of individual differences on the proposed system and a template matching method to extract IHR are also described in Sect. 3. Section 4 provides experimental results. Finally, conclusions are presented in Sect. 5.

2. Heartbeat Measurement Using Microwave Doppler Sensor

2.1 Principle of Microwave Doppler Sensor

When a radio wave is irradiated to an object, its reflected wave has a frequency shifted according to the velocity of the object. This phenomenon is known as the Doppler Effect.

Heartbeat causes minute fluctuations on the body surface. Therefore, they are visible by irradiating microwaves to the body chest because the reflected waves include a frequency shift caused by the Doppler Effect according to the velocity of the chest surface. The heart rate can also be estimated by the time interval of a slight frequency deviation caused by the pulsation. However, because the fluctuation of the chest surface is slight, high temporal resolution and spatial resolution must be used to observe the variation. In this study, a 24-GHz microwave Doppler sensor is used because the higher transmission frequency produces higher resolution.

Figure 2 shows the measured example of the microwave Doppler sensor. Then, the distance between the sensor and a subject is set to 30 cm. As presented in Fig. 2, the microwave Doppler sensor outputs Doppler waves $I(t)$ and $Q(t)$ by mixing a transmission wave $TS(t)$ and a received wave $RS(t)$. In this work, we employ a 24-GHz microwave sensor; only $I(t)$ is used to detect the heart beat. $I(t)$ can be derived from the following equation:

$$I(t) = \frac{AA'}{2} \sin\left(\frac{2V}{\lambda} \times 2\pi t\right). \quad (1)$$

Here A, A', λ, and V respectively denote the transmitted wave amplitude, the received wave amplitude, the transmitted wave wavelength, and the target object velocity (m/s). The difference between $Q(t)$ and $I(t)$ is $\pi/2$ phase delay. Although it is useful for direction estimation, only $I(t)$ is required in our system to detect the heart rate. When the

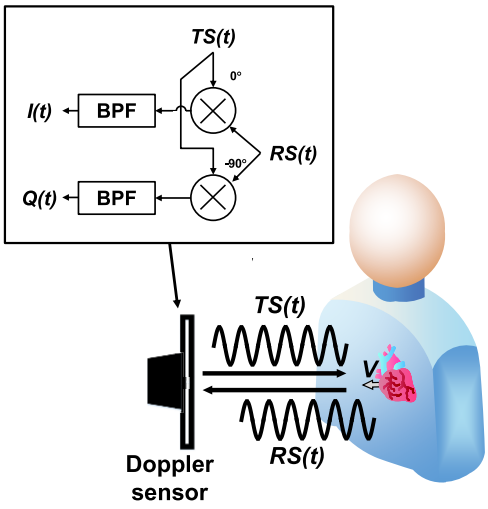

Fig. 2 Non-contact IHR detection system using microwave Doppler sensor.

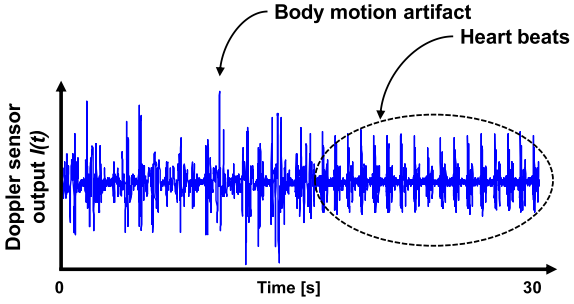

Fig. 3 Measured example of Doppler sensor output with heartbeat component and body motion artifact.

microwave is irradiated to the chest of a subject in a resting condition, the Doppler wave $I(t)$ includes information of the heart beat velocity. Therefore, the heart rate is obtainable from the Doppler wave $I(t)$.

2.2 Body Motion Artifact

When the subject is not at rest, it is difficult to detect the heart beat correctly using the time domain analysis. When the subject moves, the Doppler wave $I(t)$ is contaminated by the velocity of the human body motion, as depicted in Fig. 3. We designate this noise as a body motion artifact. If the $I(t)$ includes both the velocity of the human body motion W and the velocity of the heart beat V, then it can be explained as shown below.

$$I(t) = \frac{AA_1'}{2} \sin\left(\frac{2W}{\lambda} \times 2\pi t\right) + \frac{AA_2'}{2} \sin\left(\frac{2(W+V)}{\lambda} \times 2\pi t\right) \quad (2)$$

If the body motion velocity component W is contained in the Doppler sensor output, then heartbeat components are buried in noise and it is difficult to extract IHR in time domain as depicted in Fig. 3. However, the heartbeat component

V is also included as frequency information as shown in (2). Therefore, by performing frequency analysis, heartbeat component V and the body motion noise component W can be confirmed separately. In the following section, this report describes our examination of algorithms and the effects of parameters on frequency analysis.

3. Time-Frequency Analysis for IHR Extraction from Noisy Doppler Sensor Output

Because Doppler waves include noise caused by body motion and sensor vibration, it is difficult to detect pulsation on the time axis as shown in Fig. 3. For this study, we perform time–frequency analysis to extract feature quantities on the frequency axis to extract the heartbeat component from noisy sensor output.

3.1 Burg's Method

The shifted frequency of the Doppler wave caused by the pulsation is several hertz to several tens of hertz. Furthermore, to detect heartbeat information accurately for feature extraction, 100 ms or better time resolution is necessary because the heartbeat has short time duration. However, with FFT that is generally used in heart rate variability analysis, it is difficult to observe heart rate components having a window length of 100 ms. Therefore, we introduce an autoregressive (AR) model-based frequency analysis, which is superior for analysis of short time data. In addition, the Burg's method is used for parameter estimation of the AR model [15], [16]. Frequency analysis by the Burg's method achieves higher frequency resolution than FFT when the window length is short.

Two approaches are used for frequency analysis. Non-parametric methods produce direct power spectral density (PSD) estimate from the input signals, similarly to a fast Fourier transform (FFT). A salient benefit of this approach is that the estimated PSD is accurate. However, it requires longer input data length to maintain the frequency resolution. To obtain the IHR, a spectrogram with fine time resolution is needed. Although it can be generated from short length data, the short input data length degrades the frequency resolution. Consequently, the input data length and frequency resolution in the non-parametric methods have a tradeoff relation. The PSDs from the short-term time frequency analysis must be used to acquire the IHR. Therefore, non-parametric methods are unsuitable.

In contrast, a parametric method models the input signal as an output of white noise passed through a particular linear system (filter). Therefore, this linear system can estimate the input signal PSD. To provide frequency analysis at a higher resolution from few data, we use the parametric method.

PSD estimation is represented as the following equation.

$$\boldsymbol{P}(f) = \frac{1}{F_s} \frac{\sigma^2}{\left|1 - \sum_{i=1}^{M} \boldsymbol{a}_i e^{-j2\pi i f/F_s}\right|^2} \tag{3}$$

Here, F_s, σ^2, $\boldsymbol{a}$, and M respectively denote the sampling frequency, the expected value of the product of white noise of different times, the linear system parameter, and the order of the linear model. Bold letters denote column vectors. There are four kinds of estimation methods for this parameter; Yule-Walker AR, Burg, covariance and modified covariance method. For this study, we use Burg's method to estimate the linear system parameters. Burg's method can give higher resolution of the PSD estimate for short data than the Yule Walker AR method. Moreover, it always generates a stable model. Therefore, the measured Doppler sensor output can be separated in short windows to calculate the PSD.

3.2 Parameter Determination for Burg's Method

To obtain the accurate PSD with reasonable processing time, parameters of Burg's method should be optimized for this application. Both of the time resolution and the frequency resolution are affected by the window length, because it affects to the accuracy of the linear system parameter $\boldsymbol{a}$ in (3). The sampling frequency also affects to the accuracy because of the quantization error.

To determine the optimal order M, we use Akaike information criterion (AIC) [17] for order determination in this study. It prepares the candidates of a model that has different order, and determines the maximum log-likelihood. Then, as a correct model, it adopts a model having the largest maximum log-likelihood. However, if the order is larger, then a maximum log-likelihood also tends to increase. Therefore, in AIC, a model with large order has little likelihood of being chosen because of a penalty for large orders. AIC can be expressed as the following equation.

$$\begin{aligned} AIC \;=\; & -2(\text{Maximum log} - \text{likelihood}) \\ & + 2(\text{degree of freedom of parameter}) \end{aligned} \tag{4}$$

The degrees of freedom of the model parameters tend to be numerous in the higher order models. Therefore, the order with the smallest AIC is the optimal order. For this study, we use the following equation to calculate optimal order M.

$$AIC_i = \left(N - 2\sqrt{N}\right)(\log 2\pi + 1 + \log E) + 2(i+1) \tag{5}$$

$$M = min_{1 \le i \le N - 2\sqrt{N}} AIC_i \tag{6}$$

In (5) and (6), N and E respectively denote the length of input data and the residual variance of the model calculated using Burg's method. As shown in (6), i which minimize $AICi$ in (5) is used as an optimal model order. This AIC might vary according to the window width. As described in this paper, we compare the M of AIC with the maximum M of the window width.

Window length N, sampling frequency Fs, and model order M are evaluated in Sect. 4 using measured data.

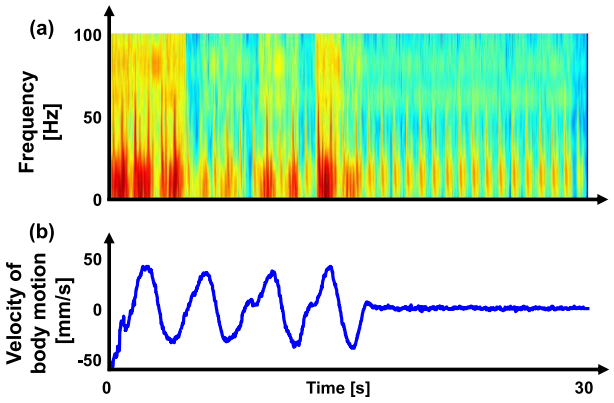

Fig. 4 (a) PSD estimated by Burg's method with 100-ms window width and (b) Simultaneously recorded velocity of body motion measured by range imagery. The same data as in Fig. 3 is used for analysis.

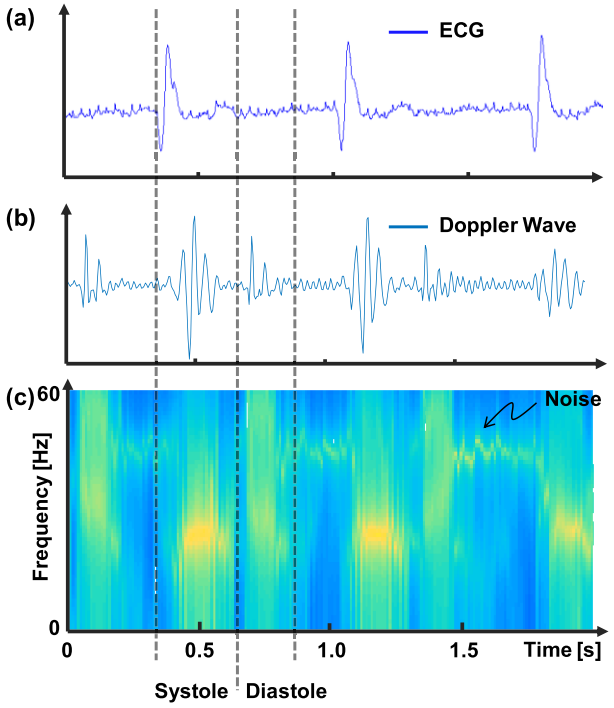

Fig. 5 Measurement example of heartbeats: (a) ECG (reference sensor), (b) microwave Doppler sensor output, and (c) PSD of Doppler sensor output.

3.3 Analysis Results of Measured Data

Figure 4 presents an example of PSD calculated by Burg's method. The time domain waveform of this data was shown in Fig. 3. In Fig. 4(b), the average velocity of body motion is simultaneously measured by a range imagery sensor. The result shows that the heartbeat components are still remaining even if large body motion artifacts are included.

Figure 5 presents a comparison of the ECG (a) and Doppler wave (b) including the heartbeat. Then, a pasted type ECG sensor [18] is used to record the ECG signal simultaneously with a microwave Doppler sensor. Figure 5(c) shows the PSD calculated from Doppler wave. As results showed, the Doppler wave can measure heartbeat components accurately, and it includes the heart contraction and expansion. The signal appearing in the frequency band of 40–50 Hz is environmental noise.

3.4 IHR Extraction Using Template Matching

Figures 4 and 5 show that the PSD calculated by Burg's method contains enough information to extract IHR. However, there are individual differences in the frequency characteristics of the heartbeat component, and it is difficult to predetermine the center frequency for IHR extraction. Thus in this research, we introduce a method to obtain IHR in time frequency domain by template matching.

Our earlier report [1] proposed an autocorrelation and a template matching method used to extract the IHR from a noisy electrocardiogram. The peak of the coefficients is appearing regularly. We can calculate the IHR from the peak coefficient intervals. In the previous work, template matching is used in one-dimension of the time domain. However, in the time-frequency domain analysis, it is difficult to decide the target frequency because the verbosity of the heart beat has different characteristics individually. It is affected by clothing, body type, and positional relation between the sensor and subjects. Therefore, this study expands this algorithm to two dimensions of the time-frequency domain. The calculation of the correlation coefficient CC between a template data and PSD at time t is expanded as following.

$$CC[t] = \sum_{i=-\frac{L_{win}}{2}}^{\frac{L_{win}}{2}-1} \sum_{f=1}^{F} TM[i][f] \cdot PSD[t+i][f] \tag{7}$$

Therein, L_{win}, F, TM and PSD respectively denote the window width, the upper limit of the frequency range, the generated template, and the PSD of Doppler sensor output. In this work, the window width and the frequency range were determined empirically as 0.5 s and 50 Hz.

4. Performance Evaluation

The performance of the IHR extraction is evaluated using measured Doppler sensor output.

We used a Doppler sensor (NJR4233D; New Japan Radio Co. Ltd.) for this experiment. Then, an ECG sensor is used as a reference sensor [18], which obtain an accurate heart rate with 1-kHz sampling rate for validation.

We calculated the root mean square (RMS) error between the reference sensor's IHR and that obtained using the proposed method. The computing time was also evaluated using Matlab 2015b (The MathWorks Inc.) running on a personal computer (3.6 GHz core i7 processor by Intel Corp. and 8 GByte working memory).

The RMS error was calculated as shown below.

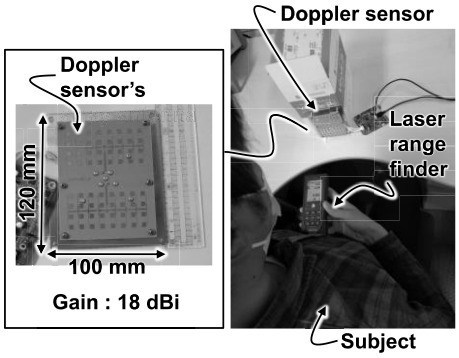

Fig. 6 Experimental setup for indoor environment.

$$\text{RMS error} = \sqrt{\frac{\sum_{t_n=1}^{N}\left(R_{IHR_{t_n}} - P_{IHR_{t_n}}\right)^2}{N}} \tag{8}$$

In that equation, N, $R_{IHR_{t_n}}$ and $P_{IHR_{t_n}}$ respectively denote the number of data of the IHR, the IHR value obtained using the reference sensor, and the value obtained using the proposed method.

4.1 Evaluation in Indoor Environment

First, we evaluated the effects of the parameters of window width N, sampling frequency Fs, order M, and the distance between the Doppler sensor and the subject. Here, the evaluation is conducted in indoor environment, which was conducted in our ordinary laboratory, not in a shielded room. The experimental setup is shown in Fig. 6. The heart rates for four men aged 22–23 were calculated. The duration of each measured data is 60 s for each subject.

Figures 7–9 respectively show the evaluation results of the sampling frequency, the window width, and the distance between the sensor and subjects. The RMS error and the processing time are affected by these parameters. We compared the RMS error performance with those reported in the literature [19] for another heart rate extraction system using an ultra-wide band Doppler sensor. Its RMS error was 5.1 ms, but its sample frequency and processing time are unknown.

Figures 7 and 8 show that the processing time and the RMS error between the reference sensor output and calculated IHR. Then, the distance between the sensor and subjects is set to 50-cm.

In Fig. 7, the sampling frequency is swept from 100 Hz to 1 kHz. The window length is set to 100 ms in this evaluation. The conventional 1-dimensional template matching is conducted with three kinds of target frequency; 30, 40, and 50 Hz. The proposed 2-dimensional template matching always improves its RMS error compared with 1-dimention template matching. The AIC can reduce the processing time of the 2-dimensional template matching, it is about 29.7% at 800 Hz sampling frequency. When the sampling rate is higher than 200 Hz, there is only 0.63 ms RMS error difference regardless of AIC in the 2-dimensional template matching.

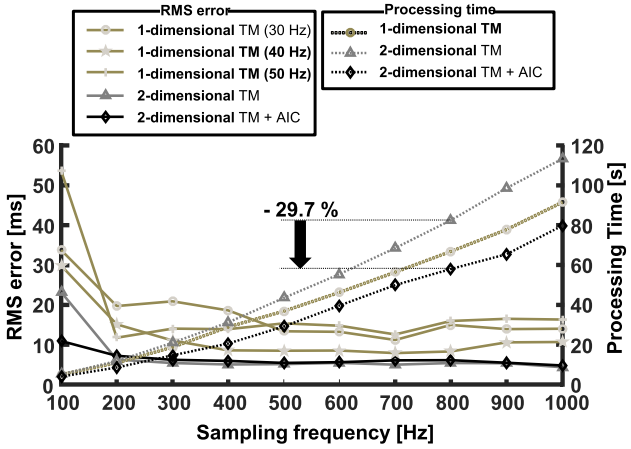

Fig. 7 Evaluation result of RMS error and processing time with 50-cm distance and 100-ms window width. Sampling rate is swept.

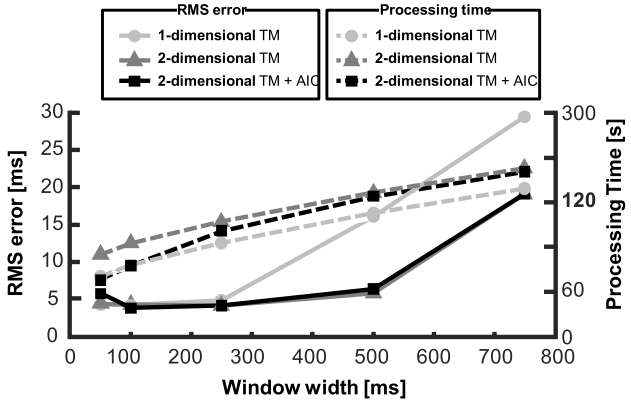

Fig. 8 Evaluation result of RMS error and processing time with 50-cm distance and 1-kHz sampling rate. Window width is swept.

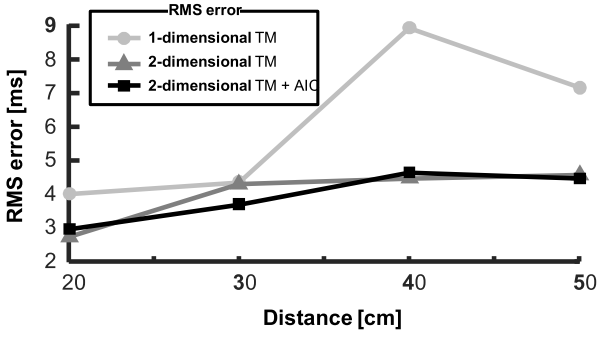

Fig. 9 Relation between RMS error and distance to subject with 1-kHz sampling rate and 100-ms window width.

In Fig. 8, the window length is swept from 50 ms to 750 ms. The sampling rate is set to 1 kHz. Although the processing time is proportionally increased according to the window length, the RMS error has optimal point. A minimum RMS error is 4.5 ms in this evaluation with 100-ms window length.

Finally, we evaluated the effect of the distance between the sensor device and subjects as shown in Fig. 9. The dis-

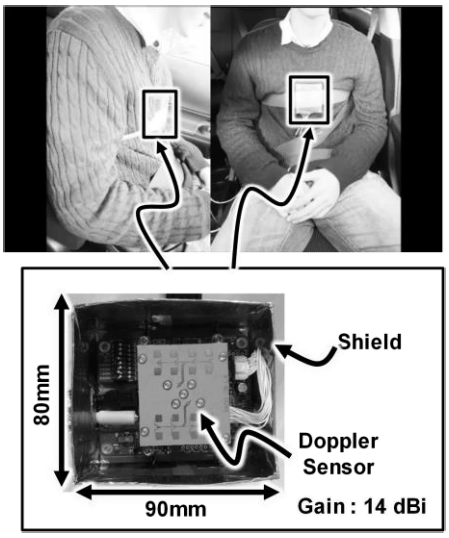

Fig. 10 Experimental setup in car.

tance is swept from 20 cm to 50 cm. The sampling rate and the window length is respectively set to 1 kHz and 100 ms. The 2-dimensional template matching with AIC shows better performance regardless of the distance. When the distance is set to 20 cm, the minimum RMS error is less than 3 ms.

4.2 Evaluation in a Car

Next, measurement experiments were carried out in the car while driving. Figure 10 shows the experimental setup. When the antenna is separated from the human body, the vibration of the vehicle is measured by irregular reflection of radio waves in the vehicle. Therefore, in this study, we assumed that the sensor is attached to the seat belt. A smaller size antenna compared to indoor experiment was used.

To evaluate the performance of the proposed method, we measured 11 participants: 9 men and 2 women who were 22–36 years old. Figures 11 and 12 respectively show the absolute error of extracted IHR, and Bland Altman plot. The evaluation is conducted using measured data for 1 minute each while driving and stopping. Table 1 shows RMS error (RMSE), absolute error (AE) and average driving speed of each subjects. As shown in this result, the proposed method achieved 13.1-ms RMS error while driving. The mean values of RMSE and AE during driving are 15.397 ms and 11.891 ms with 2 women subjects, and 12.602 ms and 9.167 ms with 9 men subjects, respectively. Some subjects have large error during stopping than during driving, because it is affected by outliers caused by sudden errors such as body movements. The influence of such errors sometimes larger than the influence of driving, because we evaluated beat-by-beat intervals instead of average heart beat interval.

In Figs. 11 and 12, conventional heart rate extraction performance shown in prior work [20] is plotted as Conv., which embedded a microwave Doppler sensor on a seat in the car. The frequency analysis based on MUSIC method is used in the conventional method, and the heart rate is calcu-

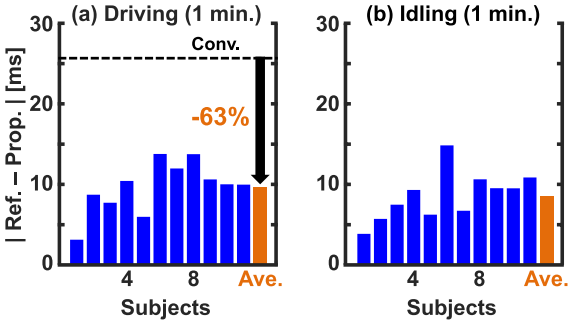

Fig. 11 Absolute error of extracted IHR while (a) driving and (b) Idling state. Each evaluation used 1-minute duration measured data. Conv. shows the conventional work [20].

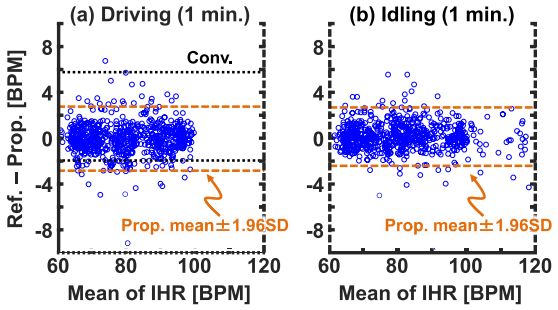

Fig. 12 Bland-Altman plot of all subjects while (a) driving and (b) Idling state. Conv. shows the conventional work [20].

Table 1 Evaluation result of RMS error (RMSE), absolute error (AE), and average speed while measurement (AS) with Each Subjects.

Subject	Driving			Stopping		
	RMSE [ms]	AE [ms]	AS [km/h]	RMSE [ms]	AE [ms]	AS [km/h]
1	3.996	3.180	46.263	5.531	3.918	0.000
2	11.622	8.745	35.078	7.709	5.767	0.000
3	9.992	7.741	43.106	9.395	7.537	0.000
4	14.048	10.448	32.483	11.194	9.355	0.000
5	8.446	6.001	39.934	11.544	6.300	0.000
6	17.331	13.783	32.259	19.113	14.883	0.000
7	18.176	11.991	43.161	9.344	6.778	0.000
8	17.458	13.759	34.073	13.111	10.669	0.000
9	16.474	10.627	40.382	12.624	9.573	0.000
10	13.337	10.023	37.591	12.334	9.566	0.000
11	13.333	9.989	37.084	15.261	10.906	0.000
Ave.	13.110	9.662	38.310	11.560	8.659	0.000

lated from the peak of PSD from 1-minute window width. The proposed method achieves 63% smaller absolute error with better 95% prediction interval in Bland-Altman plot. Furthermore, the result of conventional method is average heart rate with in 1 minute and it is not suitable for heart

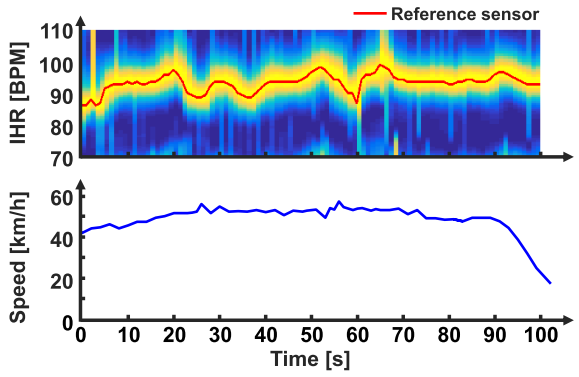

Fig. 13 Example of extracted IHR and driving speed while driving. The correlation coefficient in template matching is shown on the Z axis of the graph of IHR. The brighter color indicates stronger correlation. In addition, the IHR extracted from the reference sensor (ECG) is superimposed.

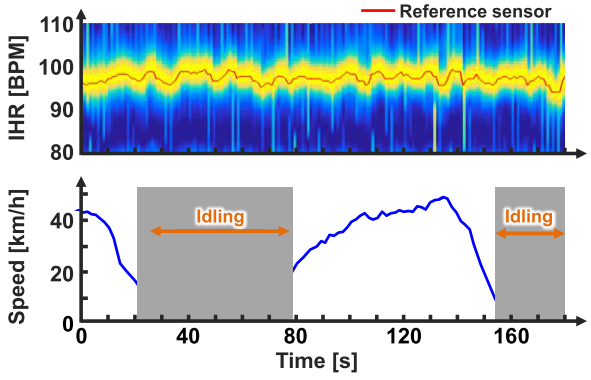

Fig. 14 Example of extracted IHR and driving speed during acceleration and deceleration. The correlation coefficient in template matching is shown on the Z axis of the graph of IHR. The brighter color indicates stronger correlation. In addition, the IHR extracted from the reference sensor (ECG) is superimposed.

rate variability monitoring. On the other hand, the proposed method shows higher accuracy, although it is evaluated with IHR per beat.

Figures 13 and 14 shows the extraction result of IHR of subject 1 for a longer period. As shown in these graphs, the IHR is correctly extracted even in during acceleration and deceleration.

Finally, we compare the accuracy of the proposed method to prior works. In literatures [20] and [21], 24-GHz microwave Doppler sensor is used to detect the heartbeat. In literature [20], it achieves 2.85-bpm AE, and its ±1.96SD are +5.64 ms and −1.98 ms with 1 subject in a car. In literature [21], 3.57-bpm AE at sitting condition and 4.06-bpm AE while typing a laptop are achieved with 5 subjects in a room. Compared with these results, the proposed method achieves smaller AE and ±1.96SD error with 11 subjects in the car. Note that the accuracy of the proposed method is evaluated by IHR from beat-by-beat intervals, although the prior works evaluated the average heart rate.

In literature [22], the accuracy of beat-by-beat interval measured by PPG sensor is discussed by comparing with ECG, and its error is almost same or larger than the proposed method. Furthermore, the influence of errors due to PPG sensor on heart rate variability analysis has been evaluated in literature [23], and the result show that the error can be accepted by removing unreliable section. Therefore, the accuracy of the proposed method is acceptable for practical applications.

5. Conclusion

To realize non-contact IHR monitoring, this paper investigated a time-frequency analysis method for microwave Doppler sensors. To clarify the performance of the proposed system, the effect of the AR model order, the window width, the sampling rate, and the distance between the Doppler sensor and subjects was evaluated with measurement data. The proposed method using time-frequency analysis and 2-dimensional template matching achieved 4.50-ms RMS error with 50-cm distance. Furthermore, the proposed method was evaluated in a car while driving with 11 subjects sitting in the passenger's seat. The evaluation results show that the proposed method can achieve 13.1 ms absolute error while driving on the ordinary road.

As a matter left for examinations in future work, body motion of the subject should be extracted from the same Doppler sensor and another filtering method. Stress and sleeping conditions can be examined by measuring both the IHR and the breathing of the subject. Possible applications can be extended to sleep state measurement, and early detection of heart disease.

Acknowledgments

This research was supported by JSPS KAKENHI Grant Number JP16H05868 and a Grant from Takata Foundation.

References

[1] S. Izumi, K. Yamashita, M. Nakano, S. Yoshimoto, T. Nakagawa, Y. Nakai, H. Kawaguchi, H. Kimura, K. Marumoto, T. Fuchikami, Y. Fujimori, H. Nakajima, T. Shiga, and M. Yoshimoto, "Normally off ECG SoC with non-volatile MCU and noise tolerant heartbeat detector," IEEE Trans. Biomed. Circuits Syst., vol.9, no.5, pp.641–651, Oct. 2015.

[2] X. Chen, X. Hu, R. Ren, Z. Bing, T. Xiao, X. Jiabai, F. Zhen, Q. Yangmin, L. Huaiyong, T. Lili, and X. Shanhong, "Noninvasive ambulatory monitoring of the electric and mechanical function of heart with a multifunction wearable sensor," Proc. IEEE COMPSACW, pp.662–667, July 2014.

[3] H.-P. Kew and D.-U. Jeong, "Wearable patch-type ECG using ubiquitous wireless sensor network for healthcare monitoring application," Proc. Second International Conference on Interaction Sciences, pp.624–630, Nov. 2009.

[4] B.-S. Lin, W. Chou, H.-Y. Wang, Y.-J. Huang, and J.-S. Pan, "Development of novel non-contact electrodes for mobile electrocardiogram monitoring system," Proc. IEEE Translational Engineering in Health and Medicine, pp.1–8, 2013.

[5] Y.M. Chi, S.R. Deiss and G. Cauwenberghs, "Non-contact low power EEG/ECG electrode for high density wearable biopotential sensor networks," International Workshop on Wearable and Implantable Body Sensor Networks, pp.246–250, June 2009.

[6] A. Tedim, P. Amorim, and A. Castro, "Development of a system for the automatic detection of air embolism using a precordial Doppler," Proc. IEEE EMBC, pp.2306–2309, Aug. 2014.
[7] A.K. Tafreshi, M. Karadas, C.B. Top, and N.G. Gencer, "Data acquisition system for harmonic motion microwave Doppler imaging," Proc. IEEE EMBC, pp.2873–2876, Aug. 2014.
[8] J.P. Phillips and P.A. Kyriacou, "Comparison of methods for determining pulse arrival time from Doppler and photoplethysmography signals," Proc. IEEE EMBC, pp.3809–3812, Aug. 2014.
[9] S. Kogelenberg, C. Scheffer, M.M. Blankenberg, and A.F. Doubell, "Application of laser Doppler vibrometery for human heart," Proc. IEEE EMBC, pp.3809–3812, Aug. 2014.
[10] C.B. Top, A.K. Tafreshi, and N.G. Gençer, "Harmonic motion microwave Doppler imaging method for breast tumor detection," Proc. IEEE EMBC, pp.6672–6675, Aug. 2014.
[11] D. Obeid, S. Sadek, G. Zaharia, and G.E. Zein, "Feasibility study for non-contact heartbeat detection at 2.4 GHz and 60 GHz," International Union of Radio Science (URSI), 2008.
[12] D. Nagae and A. Mase, "Measurement of heart rate variability and stress evaluation by using microwave reflectometric vital signal sensing," Rev. Sci. Instrum., vol.81, no.9, pp.0943011–0943014, September 2010.
[13] D. Shao, Y. Yang, C. Liu, F. Tsow, H. Yu, and N. Tao, "Noncontact monitoring breathing pattern, exhalation flow rate and pulse transit time," IEEE Trans. Biomed Eng., vol.61, no.11, pp.2760–2767, Nov. 2014.
[14] D. Matsunaga, S. Izumi, H. Kawaguchi, and M. Yoshimto, "Non-contact instantaneous heart rate monitoring using microwave Doppler sensor and time-frequency domain analysis," Proc. IEEE BIBE, pp.172–175, Nov. 2016.
[15] J.P. Burg, "Maximum entropy spectral analysis," Annual International Meeting, Soc. of Explor. Geophysics, Oct. 1967.
[16] K. VOS, "A fast implementation of Burg's method," OPUS codec, 2013.
[17] T.Y. Kim, Y.H. Noh, and D.U. Jeong, "On the use of the Akaike information criterion in AR spectral analysis of cardiovascular variability signals: A case report study," Proc. of Computers in Cardiology, Sept. 1993.
[18] CamNtech Actiwave Cardio Overview, http://www.camntech.com/products/actiwave-cardio/actiwave-cardio-overview, (accessed 16/11/2017).
[19] T. Sakamoto, R. Imasaka, H. Taki, T. Sato, M. Yoshioka, K. Inoue, T. Fukuda, and H. Sakai, "Accurate heartbeat monitoring using ultra-wideband radar," IEICE Electron. Express, vol.12, no.3, p.20141197, Jan. 2015.
[20] K.J. Lee, Ch. Park, and B. Lee, "Tracking driver's heart rate by continuous-wave Doppler radar," Proc IEEE EMBC, pp.5417–5420, Aug. 2016.
[21] C. Ye, K. Toyoda, and T. Ohtsuki, "Robust heartbeat detection with Doppler radar based on stochastic gradient approach," Proc. IEEE ICC, pp.1–6,Kansas City, MO, 2018.
[22] V. Jeyhani, S. Mahdiani, M. Peltokangas, and A. Vehkaoja, "Comparison of HRV parameters derived from photoplethysmography and electrocardiography signals," Proc IEEE EMBC, pp.5952–5955, Milan, 2015.
[23] D. Morelli, L. Bartoloni, M. Colombo, D. Plans, and D.A. Clifto, "Profiling the propagation of error from PPG to HRV features in a wearable physiological-monitoring device," Healthc. Technol. Lett., vol.5, no.2, pp.59–64, Feb. 2018.

Shintaro Izumi respectively received his B.Eng. and M.Eng. degrees in Computer Science and Systems Engineering from Kobe University, Hyogo, Japan, in 2007 and 2008. He received his Ph.D. degree in Engineering from Kobe University in 2011. He was a JSPS research fellow at Kobe University from 2009 to 2011, and an Assistant Professor in the Organization of Advanced Science and Technology at Kobe University from 2011 to 2018. Since 2018, he has been an Associate Professor in the Institute of Scientific and Industrial Research, Osaka University, Japan. His current research interests include biomedical signal processing, communication protocols, low-power VLSI design, and sensor networks. He has served as a Chair of IEEE Kansai Section Young Professionals Affinity Group, as a Technical Committee Member for IEEE Biomedical and Life Science Circuits and Systems, as a Student Activity Committee Member for IEEE Kansai Section, and as a Program Committee Member for IEEE Symposium on Low-Power and High-Speed Chips (COOL Chips). He was a recipient of 2010 IEEE SSCS Japan Chapter Young Researchers Award.

Takaaki Okano received his B.Eng. degree in Computer and Systems Engineering from Kobe University, Hyogo, Japan, in 2017. Currently, he is a master course student at Kobe University. His current research is related to wearable health-care systems.

Daichi Matsunaga respectively received his B.Eng. and M.Eng. degrees in Computer and Systems Engineering from Kobe University, Hyogo, Japan, in 2015 and 2017. His current research is related to wearable health-care systems.

Hiroshi Kawaguchi received B.Eng. and M.Eng. degrees in electronic engineering from Chiba University, Chiba, Japan, respectively, in 1991 and 1993and earned a Ph.D. degree in Engineering from The University of Tokyo, Tokyo, Japan, in 2006. He joined Konami Corporation, Kobe, Japan, in 1993, where he developed arcade entertainment systems. He moved to The Institute of Industrial Science, The University of Tokyo, as a Technical Associate in 1996, and was appointed as a Research Associate in 2003. In 2005, he moved to Kobe University, Kobe, Japan. Since 2007, he has been an Associate Professor with The Department of Information Science at that university. He is also a Collaborative Researcher with The Institute of Industrial Science, The University of Tokyo. His current research interests include low-voltage SRAM, RF circuits, and ubiquitous sensor networks. Dr. Kawaguchi was a recipient of the IEEE ISSCC 2004 Takuo Sugano Outstanding Paper Award and the IEEE Kansai Section 2006 Gold Award. He has served as a Program Committee Member for IEEE Custom Integrated Circuits Conference (CICC) and IEEE Symposium on Low-Power and High-Speed Chips (COOL Chips), and as a Guest Associate Editor of IEICE Transactions on Fundamentals of Electronics, Communications and Computer Sciences and IPSJ Transactions on System LSI Design Methodology (TSLDM).

Masahiko Yoshimoto joined the LSI Laboratory, Mitsubishi Electric Corp., Itami, Japan, in 1977. During 1978–1983 he was engaged in the design of NMOS and CMOS static RAM. From 1984, he was involved in the research and development of multimedia ULSI systems. He earned a Ph.D. degree in Electrical Engineering from Nagoya University, Nagoya, Japan in 1998. From 2000, he was a Professor of the Dept. of Electrical & Electronic System Engineering of Kanazawa University, Japan. From 2004, he was a professor of the Dept. of Computer and Systems Engineering in Kobe University, Japan. His current activities specifically emphasize research and development of ultra low power multimedia and ubiquitous media VLSI systems and dependable SRAM circuit. He holds 70 registered patents. He served on the Program Committee of the IEEE International Solid State Circuit Conference during 1991–1993. Furthermore, he served as Guest Editor for Special Issues on Low-Power System LSI, IP and Related Technologies of IEICE Transactions in 2004. He was a chair of the IEEE Solid State Circuits Society (SSCS) Kansai Chapter during 2009–2010. He is also a chair of the IEICE Electronics Society Technical Committee on Integrated Circuits and Devices from 2011–2012. He received R&D100 awards from the R&D magazine for the development of the DISP and the development of the real-time MPEG2 video encoder chipset, respectively, in 1990 and 1996. He received the 21st TELECOM System Technology Award in 2006. He is a Fellow of IEICE.